XIII International Conference on Computational Plasticity. Fundamentals and Applications
COMPLAS XIII
E. Oñate, D.R.J. Owen, D. Peric and M. Chiumenti (Eds)

CHEMO-HYGRAL MODEL FOR ASR EXPANSION AND ITS EFFECTS ON FATIGUE LIVES OF BRIDGE SLABS

Yuya Takahashi*, Yasushi Tanaka†† and Koichi Maekawa†

*†School of Engineering, The University of Tokyo
Hongo 7-3-1, 113-8656, Bunkyo-ku, Tokyo, Japan
e-mail: takahashi@concrete.t.u-tokyo.ac.jp, web page: http://concrete.t.u-tokyo.ac.jp/

††Institute of Indusrtrial Science, The University of Tokyo
Komaba 4-6-1, 153-8505, Meguro-ku, Tokyo, Japan
e-mail: yasuxi@iis.u-tokyo.ac.jp

Key words: Alkali Silica Reaction, Poro-mechanics, Confinement, Fatigue Life, Bridge Deck

Abstract. For evaluating damages of structural concrete by alkali silica reaction (ASR), an analytical platform to rationally deal with the complex interaction of multi-scale chemo-physics events is being developed. For experimental verification of the predictive model proposed, ASR expansion tests under several magnitudes of confinement are conducted and the results are compared with the multi-scale simulation. It is experimentally found that the highly deviatoric compression may bring about isotropically confined ASR expansion. The poro-mechanics based multi-phase modeling can simulate this nonlinearity by considering the quasi-hydro static pressure of created ASR gels in concrete composites and its injection into the micro-pores. The investigated models are used for assessing the fatigue lives of RC bridge decks. It is shown that fatigue life can be longer with the ASR-induced expansions.

1 INTRODUCTION

ASR is one of the major deteriorations of concrete and has been intensively studied in the past decades [1-5], but practical methods to simulate structural performances of ASR deteriorated concrete are under investigation owing to its complexity of solid concrete and ASR gel's kinematics inside pores. For instance, Saouma [6] is developing FEM models for alkali aggregate reactions with considering micro chemical reactions and trying to apply the models to structural scale. Meanwhile, the authors are developing multi-scale chemo-hygral computational system, DuCOM-COM3 [7], which can conduct 3D multi-scale analysis of structural concrete. Recently, based on the above background, the authors have been developing a model for ASR reaction and its mechanistic actions accompanying multi-directional cracking based upon Biot's solid-liquid two-phase interaction model [8,9] and non-orthogonal crack-to-crack interaction modelling [10]. The gel product is thought to be an agent to migrate inside micro pores and cracks, and the concrete constitutive law of sparse cracking is integrated with the motion of ASR gels [11]. ASR expansion tests under several grades of confinement are reported in this study and their results are used for experimental verification of the ASR modeling proposed for structural concrete. Then, the verified model is used for the fatigue life assessment of reinforced concrete (RC) bridge decks as well.

2 ASR-INDUCED EXPANSION AND EFFECTS OF UNIAXIAL CONFINEMENT

2.1 Models for ASR expansion

The proposed ASR-induced expansion model is built on the basis of poro-mechanics [12], which has been used in geotechnical engineering applications such as consolidation and liquefaction of soil foundation. The ASR-gel is treated as the medium existing among crack spaces and micro-voids. Figure 1 shows the modeling of the ASR expansion and stress distribution formations. Based on the chemical equations for ASR, the rate of ASR is formulated as a function of alkali concentration, free water amount and reactive aggregate amount (Eq. (c)). The coefficient of reaction rate k is set to 0.1×10^{-7} on the basis of the results of sensitivity analysis, and the effects of relative humidity (RH) and temperature are also considered in Eq. (d) and Eq. (e). The generated ASR-gel volume is calculated by assuming $X_2Si_2O_5(H_2O)_{8.4}$ as the ASR gel molecular formula for each alkali, X (X is Na or K)[13]; the consumed alkali amount and water amount are also calculated. It is important that the amounts of water and alkali considered when calculating the reaction rate as well as the amounts consumed are treated as global variables between the thermodynamic analytical system, DuCOM, and the 3D mesoscale structural analytical system, COM3. In DuCOM, the multi-ionic approach developed by Elakneswaran et al. [14,15] is used to compute the mass balances of sodium and potassium. Strong coupling between the material properties and the mechanical phenomena is achieved.

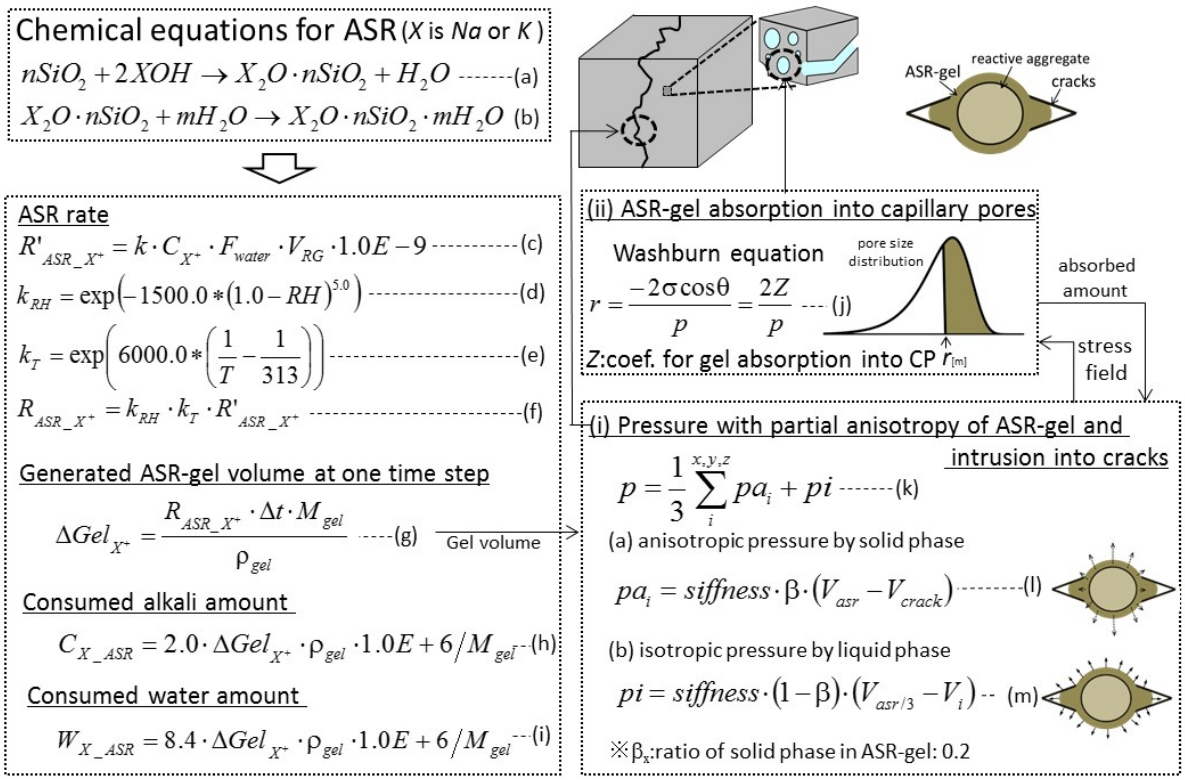

Figure 1: Chemical and Physical models for ASR

On the basis of the generated gel volume, stress formation can be calculated. However, not all created gels can be contribute to the stress formations. Some of the gel is absorbed to the capillary pores [16] and the amounts of absorbed gel can be calculated by eq. (j), which is the function of the gel pressure. Rest gels can be contribute to the stress formations. Regarding the stress calculations, we consider the semiliquid behaviors of the ASR-gels. In order to express the solid-liquid coexisting states, parameter β is introduced, which is the ratio of the solid phase to total ASR-gel. In the case of certain stress conditions, the solidified part of produced ASR-gel can expand uniformly even under anisotropic pressure distribution (Eq. (l)), while the liquid part expands without shear rigidity under isotropic pressure (Eq. (m)). The total pressure can be computed as the sum of those pressure components (Eq. (k)). Parameter β is assumed to be 0.2 for the first simple assumption with sensitivity analysis.

2.2 Uniaxial Restraint Tests

With the proposed model, simulations of uniaxial confinement tests are conducted. Experiments conducted by one of the authors [16] are referred here. Prism specimens are cast with reactive gravels, and steel bars are arranged in the longitudinal direction under several levels of steel ratios. Table 1 shows the mix proportions and experimental conditions of the experiment. The reactivity of fine aggregates was not identified by the preliminary test.

Table 1: Exprimental condition for uniaxial test

W/C [%]	W [kg/m^3]	C [kg/m^3]	S [kg/m^3]	G[kg/m^3] (reactive)	Na_2Oeq [kg/m^3]
45	169	376	775	925	8.0
Specimen size		Curing condition		Steel ratio [%]	
100*100*400mm		1day sealing → 40°C RH100%		0.0, 0.7, 1.5	

The results of length changes in the longitudinal direction in both experiments and analyses are shown in Figure 2. In the analyses, the proposed model can express drastic decreases in the length change with increasing steel ratio. The proposed models can reproduce the overall trends concerning the effects of confinement by steel.

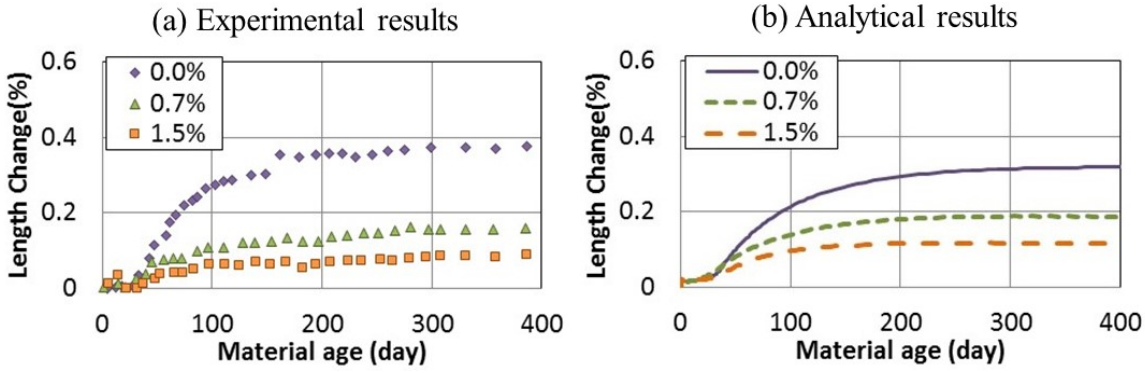

Figure 2: Chemical and Physical models for ASR

Based on the above verification, to grasp the anisotropic behaviors clearly, test with additional stress was newly conducted in this study. General conditions are shown in Table 2. Prism specimens were made with the aggregate which is reactive with alkali and additional sodium hydroxide was applied to accelerate ASR. After 28days sealed curing, specimens were subjected to three levels of confinements. The first is free expansion case, the second is the one with restraint by a ϕ13mm PC bar, and the last is the case with 6.2 MPa of additional stress by pre-stressing. After inducing these confinements, specimens were stored inside the ASR-activated environments, i.e., the temperature is kept constant at 40°C and the specimens were wrapped by wet clothes in order to supply enough water which may be consumed through ASR. Under these conditions, strains on the surfaces of the specimens and weight change were measured periodically. By using a contact-type strain gauge with chip targets attached on the specimens, space averaged strain were measured in both longitudinal and vertical directions (Figure 3).

Figure 4 shows the weight changes of the specimens. The results of three specimens are almost the same. It means that the water adsorption from wet clothes mostly coincides with each other. The degrees of ASR and the corresponding moisture states are thought to be similar among these cases.

Table 2: Exprimental condition for uniaxial and additional stress test

W/C [%]	W [kg/m^3]	C [kg/m^3]	S [kg/m^3]	G[kg/m^3] (reactive)	Na_2Oeq [kg/m^3]
55	170	309	835	983	6.1
Specimen size		Curing condition		Stress condition	
100*100*400mm		28day sealing → 40°C with wet cloths		free, restrained, additional stress	

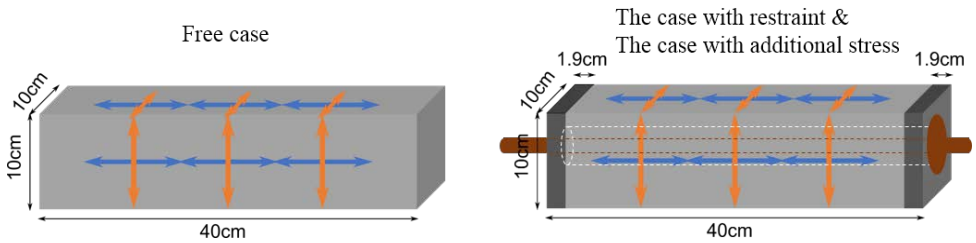

Figure 3: Dimensions of Specimens

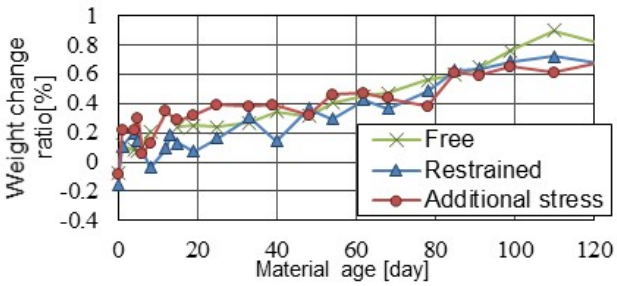

Figure 4: Weight change of specimens

Figure 5 shows the development of the strains in both longitudinal and vertical directions. The isotropic free expansion case indicates approximately 800μ by volume. With the restraint by the steel bar, significant anisotropy in expansion was observed (Figure 4 (b)). The absolute expansion is smaller than that of the free case in the longitudinal direction, while it is larger than the free case in the vertical direction. It is due to the confinement by the steel bar and such a behavior is well-known as anisotropic effect caused by liquidity of ASR gel.

The response of the case with additional compressive stresses (Figure 4 (c)) differs from the simple confinement case. Not only in the longitudinal direction but also in the vertical one, the expansion is considerably decreased in comparison with other cases. This fact cannot be simply explained only by the change of the ASR-gel movement directions. It appears that some of the generated ASR-gel is not obviously active but firmly fixed on the aggregates' surfaces. The gel adsorption into the pores of concrete mixture leads to less expansion in such a large stress conditions. This high anisotropy of deformation is similar to that of the expansive cement concrete.

Figure 6 shows the analytical results which simulate the uniaxial restraint experiments. Reactivity of aggregate or physical properties of ASR-gel cannot be identified precisely only by the reference. Then, those variables are inversely determined by sensitivity analyses using the experimental data for the free expansion case. With these parameters, the authors checked the material responses under the confinement cases.

For the case with additional stress, the analysis successfully reproduces the expansion behavior in both longitudinal and transverse directions. Without modeling the gel absorption in consideration of the gel pressure (Eq. (j) in Figure 1), such like behaviors cannot be computationally reproduced. Focusing on the amount of gel absorption in the computation (Figure 7), the absorbed amount at day 120 is about 25% larger in the additional stress case than the free one. Such difference in adsorbed amount can create the significant behavioral change in expansion. It is confirmed that the analytical model of pressure dependency of gel absorption is needed for ASR-induced expansions.

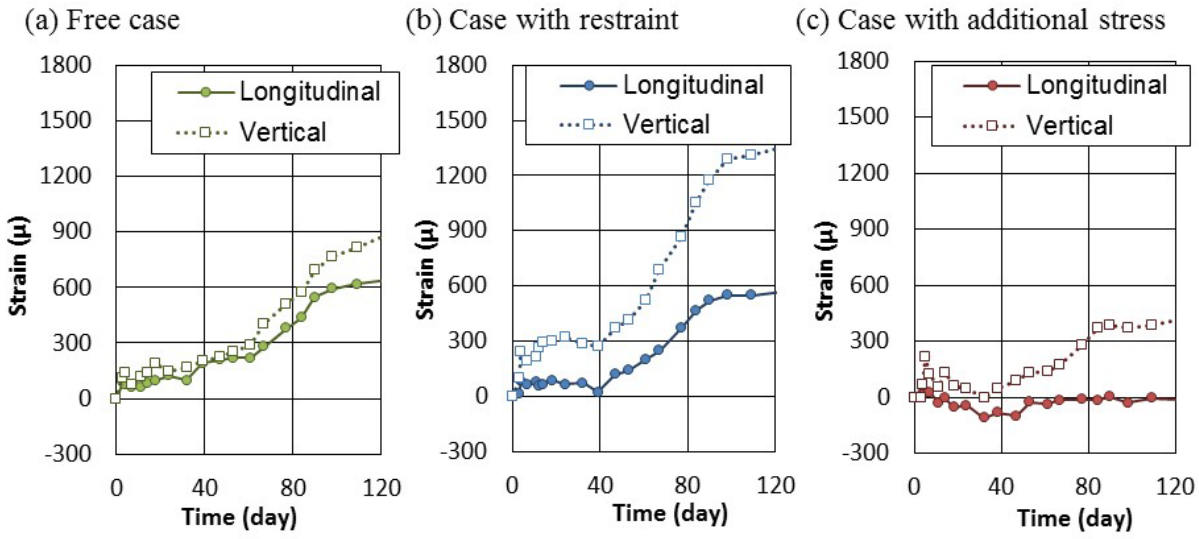

Figure 5: Measured expansions in each confinement conditions

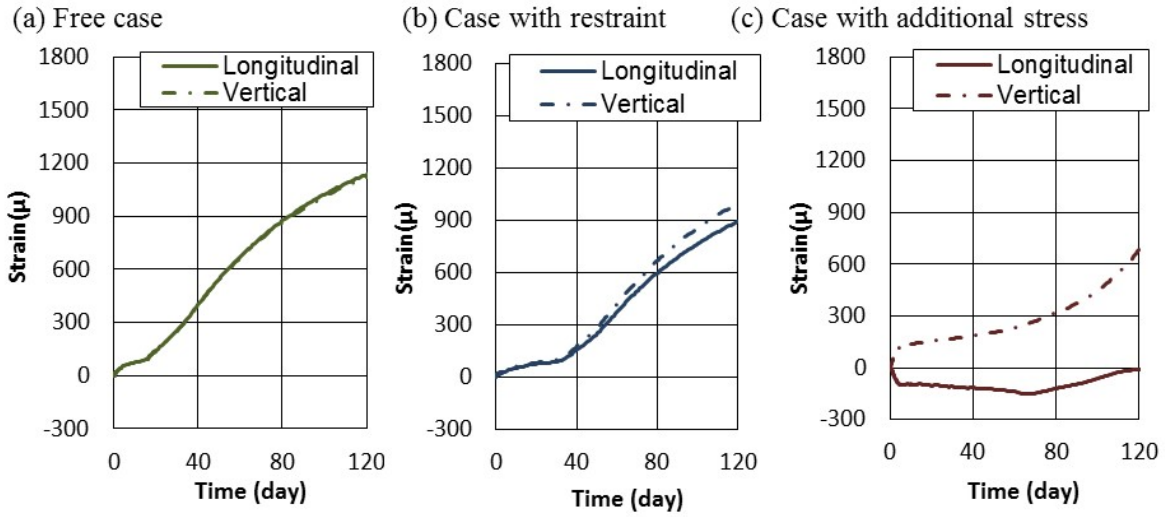

Figure 6: Calculated expansions in each confinement conditions

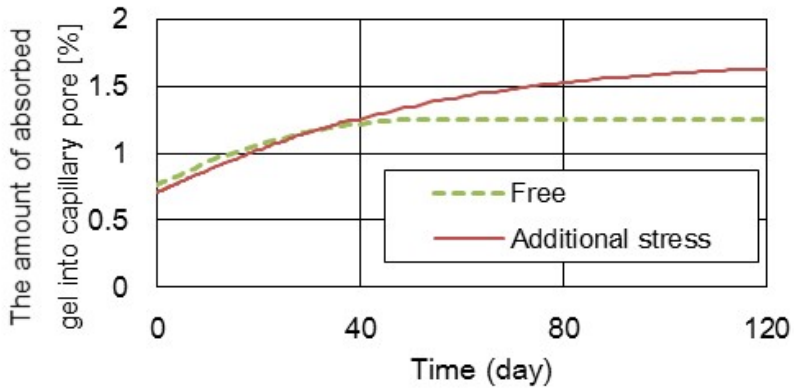

Figure 7: Gel absorption into capillary pores in calculations

For the case with simple confinement by the steel rod, the anisotropic expansion is not well simulated ((b) in Figs. 5 & 6), while such like anisotropy in uniaxial confinement experiments could be reproduced with current models in the past research by Takahashi *et al.* [11]. The difference of the past and this paper is the final expansion amount of free cases; 3500μ in the past research and 800μ in this research. Further research on the gel properties focusing on such a moderate ASR expansion cases seems to be needed.

2.3 Constant Expansion Energy Law – empirical formula -

Some researchers proposed that constant expansion energy law for the expansive cement concrete can be used also for ASR-induced concrete [17] because of their high similarity. In this study, a small discussion is added to the proposition from the analytical point of view. Assuming that concrete longitudinal strain and steel strain are the same under the uniaxial confinement conditions, constant expansion energy law can be derived from the stress-strain relationships (Eq. (1)) and the equation for expansion energy (Eq. (2)) as,

$$\sigma_{cp} = p \cdot E_s \cdot \varepsilon_{sp} = p \cdot E_s \cdot \varepsilon_{cp} \quad (1)$$

$$U = \sigma_{cp} \cdot \varepsilon_{cp} / 2 \quad (2)$$

where, σ_{cp} is the chemical pre-stress [N/mm^2], p is steel ratio, E_s is young's modulus of steel [N/mm^2], ε_{sp} is the tensile strain of steel, ε_{cp} is the expansion strain of concrete, U is the expansion energy [N/mm^2]. From these equations, expansion strain ε_{cp} can be formulated as a function of steel ratio as:

$$\varepsilon_{cp} = \sqrt{\frac{2U}{E_s}} \cdot p^{-0.5} \quad (3)$$

The expansion energy U as a materical characteristic value may differ from various material conditions, such as the amount of expansion agent, reacitivity of aggregate or amount of alkali. However, as an example, the values for U were determined as $1.47*10^3$ [N/mm^2] for the expansive cement concrete, and $2.41*10^3$ for concrete with ASR expansion, using specific experimental results in the previous study [17].

Such relations of the confined strain and the steel ratio by volume are plotted by simulating expansions under the uniaxial confinement with varying steel ratios. Analytical conditions other than steel ratios are the same as the conditions as shown in Table 1. Figure 8 shows the results of the simulations. In the figure, calculated strains with Eq. (3) under those U values are also plotted for the comparison.

Results with proposed analytical system fairly match with the results derived from the constant expansion energy law in the range of over 0.5% of steel ratio. It is shown that the proposed computational model can simulate the effects of steel ratio on ASR expansion properly and in the simple confinement conditions, constant expansion energy law seems to be empirically applicable for ASR expansion as well. This simple raw has a shortage for very less steel ratio and the computed expansion for zero confinement (free expansion) is calculated to be infinite. Then, the poro-mechanics based model can reasonably cover the whole range of steel ratio.

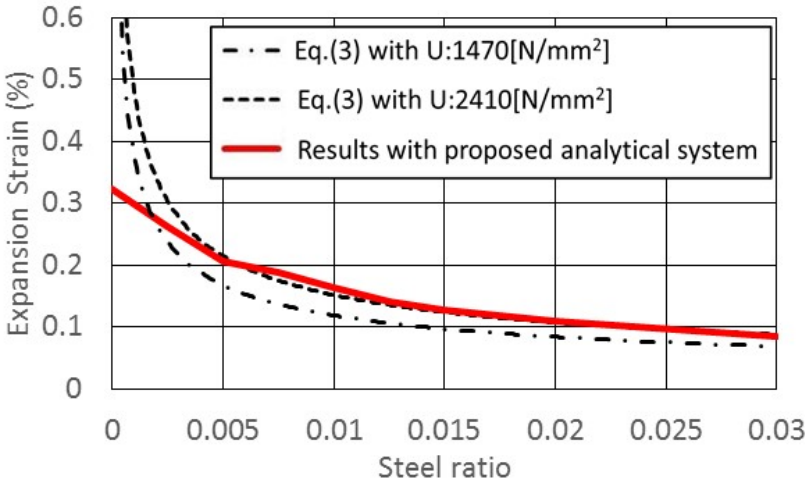

Figure 8: Strain - steel ratio relationships

3 FATIGUE LIFE ASSESMENT OF BRIDGE DECK

In this section, the proposed models are applied to the structural scale. In the previous study, applicability of the model for the beam shaped members was already shown [11]. In this study, the analytical system is tried to be used for the assessment of the fatigue lives of the reinforced concrete bridge deck slabs.

Target shape of RC slab and its analytical dimension are shown in Figure 9. Taking advantage of symmetry, only halves of the slabs are modelled. With this dimensions of RC slab, for non-ASR case, fatigue behavior with wheel type moving load are already studied and the accuracy of the analytical system was verified by Hiratsuka *et al.* [18]. So, with this RC slab, we can discuss the effect of ASR expansion on the fatigue life by comparing the behaviors during with and without ASR expansion.

In the simulations, moving loads of 16kN are applied with 3km/h of speed along the longitudinal directions at the center of the slabs and the tire/ground friction area is 300 mm wide and 450 mm long. For the ASR case, 300μ of free ASR expansion was induced in 130 days before the loading step. As a result, expansions are about 1200μ in the transverse vertical direction and about 200μ in the in-plane horizontal direction due to the confinement by the dispersed reinforcing bars.

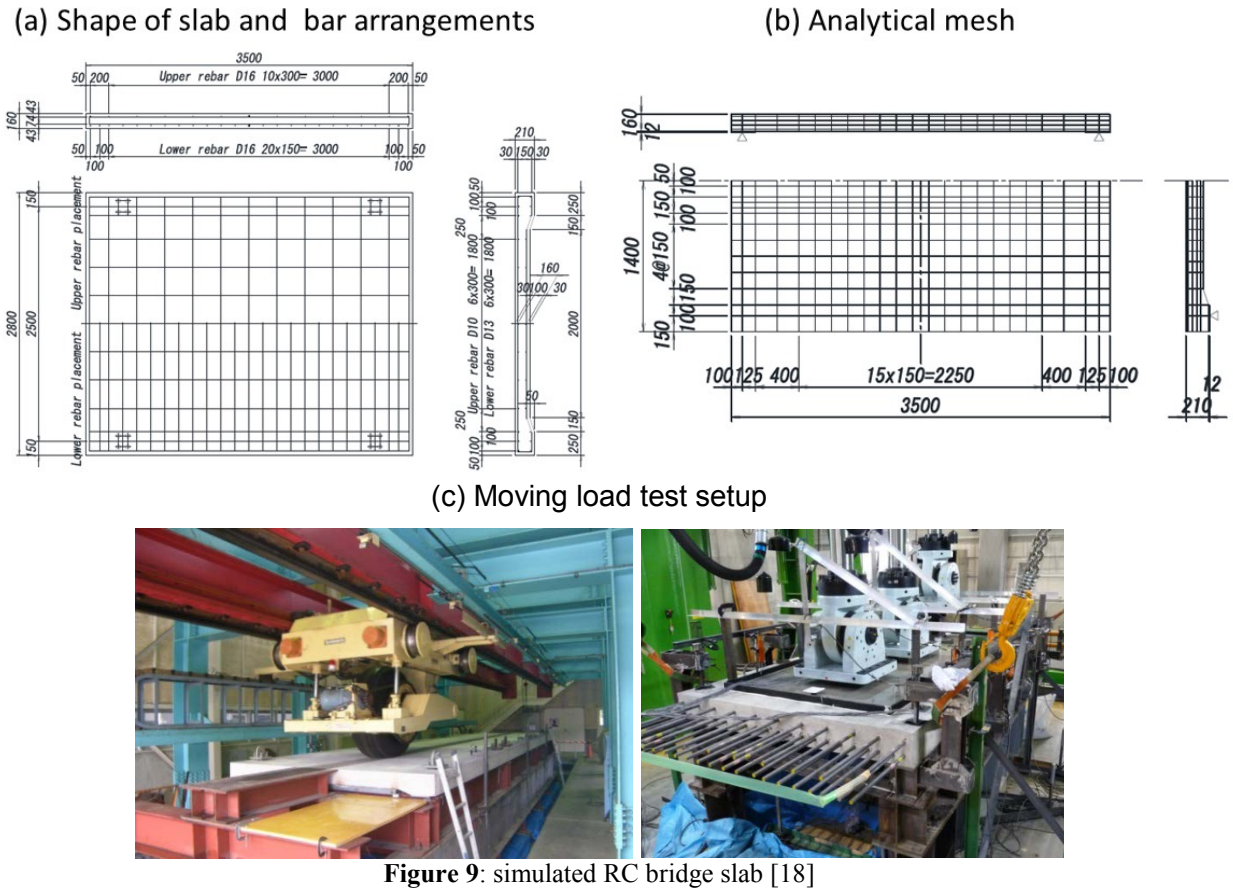

Figure 9: simulated RC bridge slab [18]

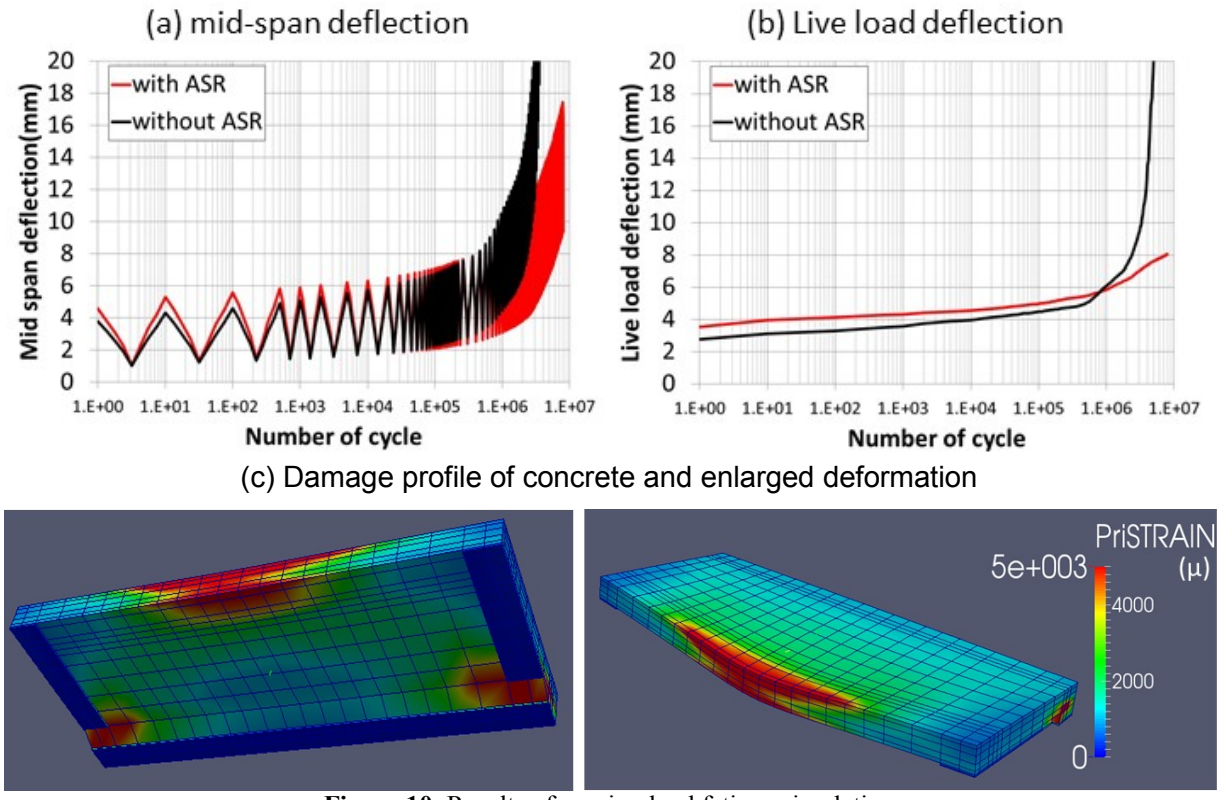

Figure 10: Results of moving load fatigue simulation

Figure 10 (a) shows the total mid-span deflections along cyclic moving loads and Figure 10 (b) is the live load deflection extracted from Figure10 (a). It can be seen that the fatigue life in the ASR case seems to be longer than no-ASR case despite ASR expansions and deteriorations (large number of multi-directional cracking induced) have occurred in the slab. One of the causes of the life extension with ASR may attribute to the chemical pre-stressing. Regarding the live load deflection, the initial value is larger in the case of ASR, but after 10^6 cycles of loads, non-ASR case has larger deflection and failed earlier.

Such a qualitative tendency in terms of the fatigue life is experimentally indicated by Maeshima *et al* [19] as well. Figure 11 shows the shape of their RC slab specimens. The slabs were cast with reactive gravels, and W/C was set to be 65%. Three different levels of ASR expansions are prepared; Case I is no ASR acceleration case, Case II has 41days of ASR acceleration (50°C, RH80%, saturated sodium chloride solution is kept on the upper surface of the slab) and expansion of 2800μ in the vertical and 800μ in the horizontal direction were appeared. Case III has environmental conditions of 87 days in 5% sodium chloride solutions and 59 days of ASR acceleration. Expansive strains of Case III reached 4900μ in the vertical and 700μ in the horizontal directions. Moving load was applied to those slab specimens by using the wheel-type fatigue loading machine. Only in Case III, water was supplied on the slabs during loading to see the effect of water on fatigue life.

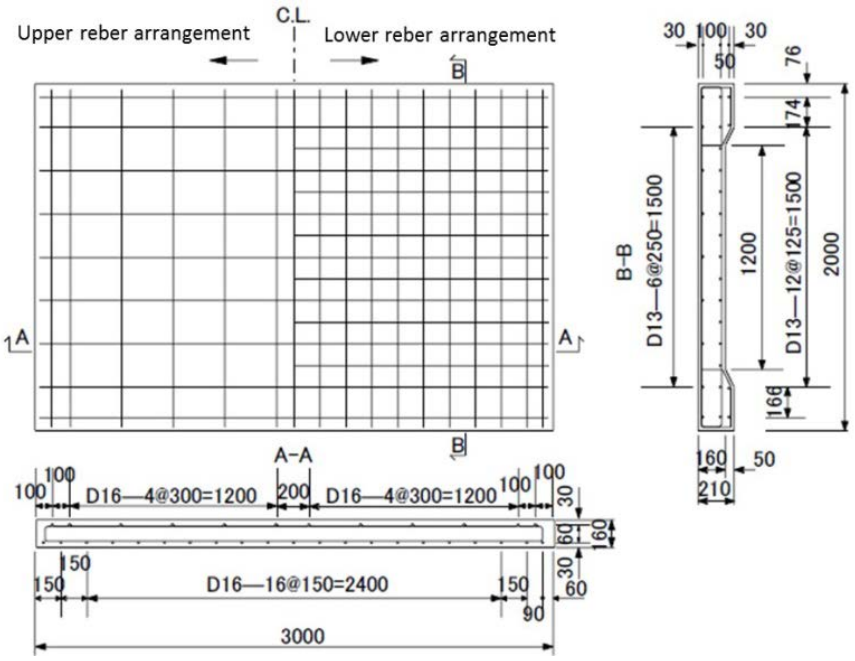

Figure 11: experimented RC bridge slab [19]

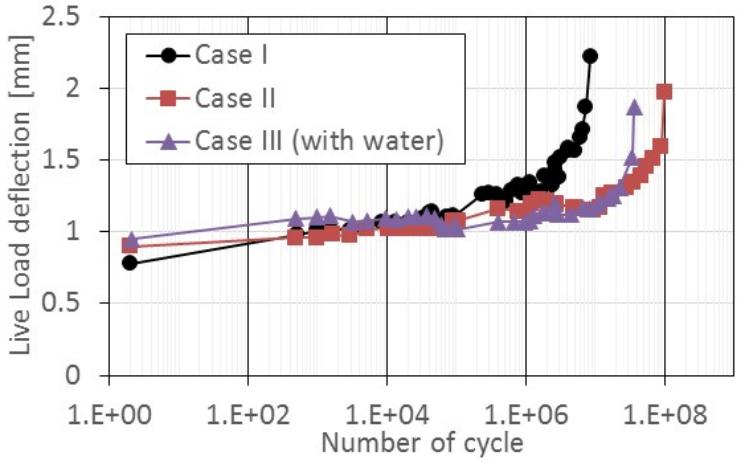

Figure 12: experimented RC bridge slab [19]

Figure 12 shows the results of Maeshima's experiments [19] and the results are similar to the analytical ones as shown in Figure 10. Though the live load deflection at the first cycle in ASR case (Case II) is larger than no-ASR case (Case I), fatigue life is 1 order longer in the ASR case than non-ASR. It was mentioned that chemical pre-stress can partly restrain the increase in live load deflections. From these analytical and experimental studies, it can be suggested that ASR has not necessarily negative effect on the structural performance of RC slabs, although the critical impacts to the structural performances have been reported such as rupture of bent reinforcing bars [20].

Fatigue life of Case III seems to be shorter than Case II as shown in Figure 12. In Case III, water was supplied on the slabs and it is known that condensed water can reduce the fatigue

life dramatically [8]. In future, the effects of other factors rather than ASR expansion, i.e. liquid water, concrete drying shrinkage, etc. and interacting effects of those factors should be investigated to predict the fatigue behaviors of concrete based bridge decks suffered by complex deteriorations. The prediction of the future remaining life is critical to steer the asset management of bridge infrastructures.

4 CONLCUSIONS

In this study, analytical models for simulating ASR-induced expansion of reinforced concrete are verified with uniaxial confinement test. To clarify the stress-induced anisotropy of the ASR expansion, additional transverse stresses are applied in the uniaxial test in compression. As a result of the experiments, observed are significant behaviors where expansive strains are restrained not only in longitudinal direction along the main steel bars but also in the transverse directions. Such an anisotropic trends can be well-simulated by the proposed models and the applicability of the models are examined quantitatively.

Furthermore, the model is applied for the fatigue life simulations of RC bridge slabs. Comparing the results of mockup decks with and without ASR-induced expansions, it is shown that ASR expansion has not necessarily negative effect on the structural performance of RC slabs, but brings about extension of fatigue life. Such tendency is found in the previous experimental studies as well.

The scope of this study is limited and a few particular cases have been investigated. Thus, so called interactive effects of ASR expansion, liquid water, and concrete shrinkage are to be more investigated in both experimental and analytical manner in future.

ACKNOWLEDGEMENTS

This study was financially supported by JSPS KAKENHI Grant No. 15H05531 and Cross-ministerial Strategic Innovation Promotion Program (SIP).

REFERENCES

[1] Bažant, Z. P. and Steffens, A. Mathematical model for kinetics of alkali-silica reaction in concrete, *Cement and Concrete Research* (2000) **30**:419-428

[2] Bangert, F., Kuhl, D. and Meschke, G. Chemo-hygro-mechanical modelling and numerical simulation of concrete deterioration caused by alkali-silica reaction, *International Journal for Numerical and Analytical Methods in Geomechanics* (2004) **28**:689-714

[3] Multon, S., Sellier, A. and Cyr, M. Chemo-mechanical modeling for prediction of alkali silica reaction (ASR) expansion, *Cement and Concrete Research* (2009) **39**:490-500

[4] Hashimoto, T. and Torii, K. The Development of Highly Durable Concrete Using Classified Fine Fly Ash in Hokuriku District, *Journal of Advanced Concrete Technology* (2013) **11**: 312-321

[5] Mohammed, T. U. Hamada, H. and Yamaji, T. Relation between Strain on Surface and Strain over Embedded Steel Bars in ASR Affected Concrete Members, *Journal of Advanced Concrete Technology* (2003) **1**:76-88

[6] Saouma, V. E. *Numerical Modeling of AAR,* CRC press (2014)

[7] Maekawa, K., Ishida, T. and Kishi, T. *Multi-Scale Modeling of Structural Concrete*,

Taylor and Francis (2008)
[8] Meakawa, K. and Fujiyama, C. Rate-dependent model of structural concrete incorporating kinematics of ambient water subjected to high-cycle loads, *Engineering Computations* (2013) **30**, Iss: 6, 825-841
[9] Biot, M. A. Theory of stability and consolidation of a porous media under initial stress, *Journal of Mathematics and Mechanics* (1963), **12(2)**:521-541.
[10] Maekawa, K., Pimanmas, A. and Okamura, H. *Nonlinear Mechanics of Reinforced Concrete*, Taylor & Francis (2003)
[11] Takahashi, Y., Shibata, K. and Maekawa, K. Chemo-hygral modeling and structural behaviors of reinforced concrete damaged by alkali silica reaction, *Proceedings of ACF2014* (2014):1274-1281
[12] Takahashi, Y., Shibata, K. and Maekawa, K. Chemo-Hygral Modeling of Structural Concrete Damaged by Alkali silica Reaction, *Proceedings of the 1st Ageing of Materials & Structures 2014 Conference* (2014):424-431
[13] Ichikawa, T. and Miura, M. Modified model of alkali silica reaction, *Cement and Concrete Research* (2007) **37**:1291-1297
[14] Elakneswaran, Y. and Ishida, T. Development and Verification of an Integrated Physicochemical and Geochemical Modelling Framework for Performance Assessment of Cement-Based Magterials, *Journal of Advanced Concrete Technology* (2014) **12**: 111-126
[15] Elakneswaran, Y. and Ishida, T. Integrating physicochemical and geochemical aspects for development of a multi-scale modeling framework to performance assessment of cementitious materials, *Multi-scale Modeling and Characterization of Infrastructure Materials, RILEM BOOKSERIES* (2013) **8**:63-78
[16] Muranaka, M. and Tanaka, Y. Development of physical and chemical model for concrete expansion due to ASR based on reaction mechanism, *Journal of JSCE* (2013) **E2/V-69, No.1**:1-15
[17] Japan Society of Civil Engineers, *Concrete Library 124, State-of-the-Art Report on the Countermeasures for the Damage Due to Alkali-Silica Reaction* (2005):II116-II118
[18] Hiratsula, Y. and Maekawa, K. The influence of Drying Shrinkage on the Fatigue Life of RC Slabs, *AMS'14 Proceedings of the International Conference on Ageing of Materials & Structures* (2014):362-369
[19] Maeshima, T., Koda, Y., Iwaki, I., Ota, K., Ono, A., Kishi. Y. and Kubo, Z. Fatigue resistance assessments of RC bridge decks deteriorated by ASR, *Proceedings of JSCE* (2014) **69**: 1221-1222 (in Japanese)
[20] Japan Society of Civil Engineers, *Concrete Library 124, State-of-the-Art Report on the Countermeasures for the Damage Due to Alkali-Silica Reaction* (2005):I26-I31